Micromagnetic simulation of magnetization reversal in small particles with surface anisotropy

W. Scholz,[a] D. Suess, T. Schrefl, and J. Fidler
Vienna University of Technology, Wiedner Hauptstrasse 8-10/138, A-1040 Vienna, Austria

(Presented on 7 January 2004)

In order to study the effect of surface anisotropy, we have developed a three-dimensional finite element micromagnetic model. The finite element mesh of the particles is split into a core region with bulk properties and a surface region (shell) of variable thickness with modified material parameters. We have studied the magnetization reversal in FePt nanoparticles. The effect of surface anisotropy strongly reduces their coercivity. An Fe–oxide shell with low anisotropy in the plane of the surface has been considered as well as surface anisotropy with high anisotropy constants and axis orientation perpendicular to the surface. © *2004 American Institute of Physics.*
[DOI: 10.1063/1.1689612]

I. INTRODUCTION

High density magnetic storage media require tight control of the grain size, grain size distribution, chemical composition, and microstructure to ensure the thermal stability of the bits and keep the media noise low. However, as the areal density increases, the grain size and the magnetic switching volume need to decrease and the surface to volume ratio increases. Thus, surface effects become more and more important for the properties of magnetic nanoparticles.

In order to maintain the stability materials with higher uniaxial anisotropy than the common CoCrPt alloys are required. FePt thin films[1] and self assembled nanoparticles[2] are promising candidates for high density magnetic storage media.[3,4] Their magnetocrystalline anisotropy is 50–100 times larger than in CoCrPt media alloys which may allow areal densities in the Tbit/in^2 regime.

II. THE FINITE ELEMENT MODEL

The numerical computer simulations have been carried out using a three dimensional hybrid finite element/boundary element micromagnetic code[5] with a magnetic scalar potential for the calculation of the demagnetizing field and a limited memory variable metric algorithm (quasi-Newton method) for minimization of the total energy.[6,7] The total energy consists of the contributions from the magnetocrystalline anisotropy energy, exchange, magnetostatic, and Zeeman energy.

III. POLYCRYSTALLINE FePt NANOPARTICLES

We have assumed a simple geometry with a hexagonal basis and a particle diameter between 15 and 120 nm with constant aspect ratio (diameter/height) of 3. The following material parameters for FePt have been assumed:[4,8] $K_V = 7.7$ MJ/m^3, $J_s = 1.43$ T, and $A = 10^{-11}$ J/m, where K_V denotes the magnetocrystalline anisotropy constant, J_s the saturation polarization, and A the exchange constant. The particle has been split into six different parts (according to its hexagonal shape) in which the orientation of anisotropy axes has been varied. In addition a surface shell of variable thickness surrounding the core of the particle has been defined to introduce surface anisotropy. Figure 1 shows an exploded view of the model.

The influence of the magnetostatic field has been shown to be negligible[9] (as compared to the anisotropy field) and has been omitted in all simulations, since the nucleation field (i.e. the coercive field of these particles) is reduced by less than 5%.

IV. OXIDIZED SURFACE SHELL

The magnetic properties of the surface of FePt nanoparticles can be altered by oxidation. Fe_3O_4 and other oxidation states have been found by near edge x-ray absorption fine

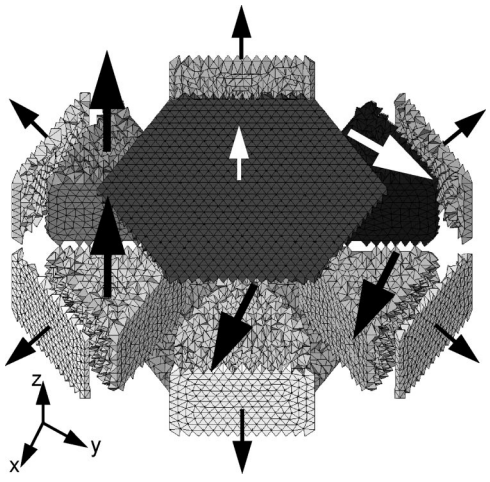

FIG. 1. Exploded view of the finite element model of a FePt nanoparticle with hexagonal basis, six inner parts, and eight surface parts. The big arrows indicate the anisotropy axes of the inner parts in the ''2:2:2'' configuration and the smaller arrows indicate those for the surface shell (perpendicular to the surface). The roughness on the interior interfaces is caused by the structure of the finite element mesh.

[a]Author to whom correspondence should be addressed; electronic mail: werner.scholz@tuwien.ac.at ⟨http://magnet.atp.tuwien.ac.at/scholz/⟩

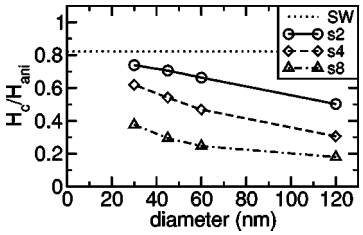

FIG. 2. Coercivity (in units of the anisotropy field $H_{ani}=2K_V/J_s$) as a function of particle diameter for a particle with a single anisotropy axis and reduced surface anisotropy (γ-Fe_3O_4 material parameters with in-plane anisotropy). The anisotropy axes in all six core parts are parallel to the z axis; "SW" indicates the switching field of a Stoner–Wohlfarth particle for an external field applied at 3° from the anisotropy axis; $s2-s8$ stands for the thickness of the surface shell as given in Table I.

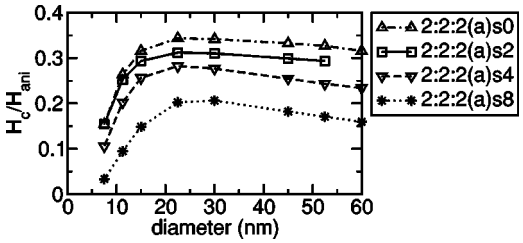

FIG. 3. Coercivity as a function of particle diameter for different thicknesses of the surface shell ($s0$ gives the results without an oxide shell). A polycrystalline particle with 2:2:2 configuration of the magnetocrystalline anisotropy axes has been assumed (cf. Fig. 1).

structure spectroscopy,[10–12] which indicates oxide shells of ≈ 0.4 nm around FePt nanoparticles measuring 4–6 nm in diameter.

Therefore, the properties of γ-Fe_3O_4[13] have been assumed for the surface shell surrounding the FePt core: $K_1 = -0.011$ MJ/m^3, $J_s = 0.5$ T, and $A = 1.32\times 10^{-11}$ J/m.

Figure 2 shows the coercive field of a uniaxial particle with $s2$ surface configuration (cf. Table I) with in-plane anisotropy in each facet. The external field is applied at an angle of 3° with respect to the anisotropy axis (which is parallel to the sixfold symmetry axis). As the particle size is reduced the thickness of the soft oxide shell is scaled down and its influence diminishes, which makes the coercivity converge to the Stoner–Wohlfarth limit.

The oxide on the surface makes the nucleation process easier due to its reduced anisotropy. As a result, the coercivity is considerably reduced as compared to the Stoner–Wohlfarth result. For very small particles the surface shell is very thin and it cannot support the nucleation process effectively. As the size of the particle is scaled up, the thickness of its surface shell increases in our model, too. This makes the nucleation process easier and reduces the coercivity.

If misaligned anisotropy axes are introduced, as indicated in Fig. 1, the coercivity is strongly reduced.[9] This is due to the fact that the misaligned parts create 90° domain walls at their interfaces. Thus, the magnetization reversal mechanism changes from nucleation (for single crystals) to domain wall pinning. The oxide shell contributes to this effect and leads to a further reduction, as shown in Fig. 3. In single crystals the oxide shell provides the nucleation site, whereas in the case of multiple easy axes it supports the domain wall depinning from the interface. This gives rise to the maximum of the coercivity as a function of the particle size as shown in Fig. 1.

TABLE I. Thickness t_s and volume of the surface shell V_{shell} in comparison with the core volume V_{core} for a particle diameter of 60 nm.

Symbol	t_s (nm)	V_{shell} (nm^3)	V_{core} (nm^3)	V_{shell}/V_{core}
$s2$	1	8000	38 000	0.21
$s4$	2	16 000	30 000	0.53
$s8$	4	29 000	17 000	1.71

V. SURFACE ANISOTROPY

If we assume strong surface anisotropy for FePt nanoparticles,[14] effective anisotropy values as high as $K_{eff} = K_S/t = 46.2$ MJ/m^3 may arise in the surface shell, where t indicates its thickness. This corresponds to a ratio $K_{eff}/K_V = 6$. As a result, we find a strongly disturbed magnetization distribution as shown in Fig. 4 for a uniaxial FePt nanoparticle with a diameter of 45 nm and a surface layer thickness of 1.5 nm.

The influence of the surface anisotropy on the coercivity of uniaxial FePt nanoparticles is shown in Fig. 5. For small particle sizes (but still large as compared to the exchange length) the coercivity approaches the nucleation field, because the thickness of the shell is on the order or below the domain wall thickness. As the particle size (and the shell thickness) increase, the coercivity is reduced by 50%. The disorder in the magnetization distribution on the surface of the particle facilitates the nucleation process and reduces the coercivity. For large particles the reduced coercity remains

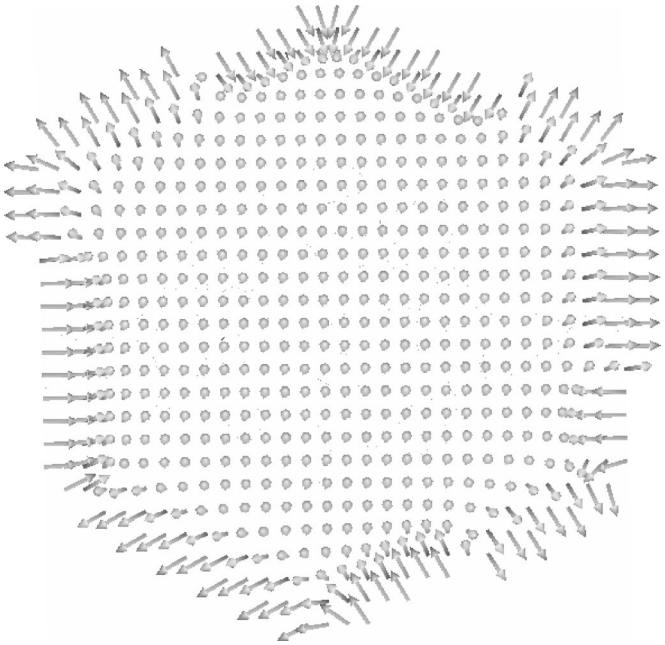

FIG. 4. Remanent magnetization configuration of a uniaxial FePt nanoparticle with a diameter of 45 nm with effective surface anisotropy $K_{eff}/K_V = 6$ and a surface layer thickness of 1.5 nm. The arrows indicate the magnetization distribution in a cut plane parallel to the hexagonal faces through the center of the particle.

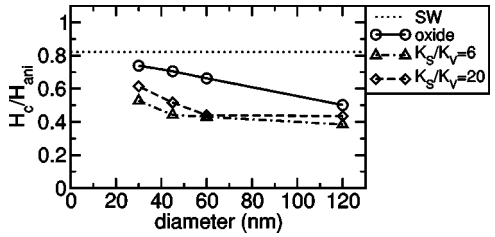

FIG. 5. Coercivity as a function of particle diameter for an oxide shell with reduced anisotropy in comparison with strong surface anisotropy. A thin shell (*s*2) has been assumed.

constant, because the nucleation process does not depend on the particle size, when the thickness of the shell is larger than the domain wall size.

For particles with a diameter on the order of a few nanometers, Monte-Carlo simulations have shown this competition between surface and bulk anisotropy, which leads to throttled and ''hedgehog'' spin structures.[14]

VI. CONCLUSIONS

We have studied the influence of core/shell configurations on the coercivity of FePt nanoparticles using micromagnetic simulations. Surface oxidation during the processing of FePt nanoparticles can lead to the formation of Fe–oxides with reduced magnetocrystalline anisotropy. The simulations show a reduction of the coercivity up to 75% depending on the particle size and thickness of the oxide shell. A similar effect is observed for ''pure'' FePt nanoparticles due to intrinsic surface anisotropy. Strong surface anisotropy perpendicular to the surface facilitates the nucleation and magnetization reversal, which leads to a similar reduction of the coercivity.

ACKNOWLEDGMENT

This work is supported by the Austrian Science Fund—Grant No. FWF P14899-PHY.

[1] S. Sun, C. B. Murray, D. Weller, L. Folks, and A. Moser, Science **287**, 1989 (2000).
[2] B. Bian, D. E. Laughlin, K. Sato, and Y. Hirotsu, J. Appl. Phys. **87**, 6962 (2000).
[3] D. Weller and A. Moser, IEEE Trans. Magn. **35**, 4423 (1999).
[4] D. Weller, A. Moser, L. Folks, M. E. Best, W. Lee, M. F. Toney, M. Schwickert, J.-U. Thiele, and M. F. Doerner, IEEE Trans. Magn. **36**, 10 (2000).
[5] W. Scholz, J. Fidler, T. Schrefl, D. Suess, R. Dittrich, H. Forster, and V. Tsiantos, Comput. Mater. Sci. **28**, 366 (2003).
[6] D. Suess, V. Tsiantos, T. Schrefl, J. Fidler, W. Scholz, H. Forster, R. Dittrich, and J. J. Miles, J. Magn. Magn. Mater. **248**, 298 (2002).
[7] S. Benson, L. C. McInnes, J. J. Moré, and J. Sarich, TAO home page ⟨http://www-unix.mcs.anl.gov/tao/⟩ (2001).
[8] T. Klemmer, D. Hoydick, H. Okumura, B. Zhang, and W. A. Soffa, Scr. Metall. Mater. **33**, 1793 (1995).
[9] W. Scholz, J. Fidler, T. Schrefl, D. Suess, H. Forster, R. Dittrich, and V. Tsiantos, J. Magn. Magn. Mater. (in press).
[10] S. Anders *et al.* Microelectron. Eng. **61–62**, 569 (2002).
[11] S. Anders, M. F. Toney, T. Thomson, R. F. C. Farrow, J.-U. Thiele, and B. D. Terris, Technical Report No. SLAC-PUB-9989, SLAC-Stanford Linear Accelerator Center, 2003.
[12] S. Anders, M. F. Toney, T. Thomson, and J.-U. T. B. D. Terris, Technical Report No. SLAC-PUB-9994, SLAC-Stanford Linear Accelerator Center, 2003.
[13] L. L. Afremov and A. V. Panov, Phys. Met. Metallogr. **86**, 269275 (1998).
[14] Y. Labaye, O. Crisan, L. Berger, J. M. Greneche, and J. M. D. Coey, J. Appl. Phys. **91**, 8715 (2002).